PHYSICAL REVIEW A **72**, 050702(R) (2005)

Random-phase approximation with exchange for the inner-shell electron transitions

Zhifan Chen and Alfred Z. Msezane
Center for Theoretical Studies of Physical Systems and Department of Physics, Clark Atlanta University, Atlanta, Georgia 30314, USA
(Received 15 June 2005; published 7 November 2005)

We present our recently developed random-phase approximation with exchange (RPAE) method, which can be used to study the inner-shell electron transition in an open-shell atom. The expressions for the matrix elements of all terms of the dipole and Coulomb interactions have been derived and implemented in a computer program. The photoionization cross sections of the $4d$ giant resonances of Xe^+, I, and I^+ have been calculated. The results for Xe^+ and I^+ agree very well with the experimental data. However, the theoretical results for the I $4d$ cross section are still almost three to four times higher than the experimental data. We recommend a remeasurement of the I $4d$ giant resonance with a careful experimental arrangement.

DOI: 10.1103/PhysRevA.72.050702 PACS number(s): 32.80.Fb, 31.25.Eb

The random-phase approximation with exchange (RPAE) method has been successfully used in photon (electron) atom (ion) collisions for quite some time. These studies demonstrated the important influence of the virtual excitation of pairs of electrons and the necessity of including these electron correlations into the calculation in order to obtain good agreement between the theoretical results and the experimental data. However, these studies have been limited mostly to the noble gases and a few other systems, as it was originally developed for the systems, with nondegenerate ground states.

The generalization of the RPAE to atoms with unfilled shells is a difficult problem and has only been performed by a few scientists. Dalgaard [1] extended the RPAE method to the calculation of oscillator strengths for the discrete transitions of open-shell atoms with two electrons or two vacancies in the valence shell (e.g., silicon). Armstrong [2], and Starace and Armstrong [3], developed a generalization of the RPAE based on the solution of Rowe equations of motion [4]. However, this generalization does not yield the equation for the filled shell in the limiting case. None of the above methods has proven that the photoionization cross sections are the same in the length and velocity forms. This problem has been resolved by Cherepkov *et al.* [5] and Vesnicheva *et al.* [6]. In the limiting case of an atom with filled shells, their method yields the well-known equation of the RPAE. Another advantage of this method is that the dipole sum rule holds. The computer code developed for the RPAE method of single open-shell atoms using Cherepkov's equations can be found in [7]. However, the code has not implemented all the parameters contained in the Cherepkov formulas. To date the RPAE method still cannot be used to study the general inner-shell electron transition of an open-shell atom except a few elements, such as I^{2+}, Cr, etc., which can be treated with the spin-polarized technique of the RPAE method.

In this paper we present our recently developed RPAE method, which can be used to study the photoionization of an inner-shell electron transition in an open-shell atom or ion. Since the computer program has been written to perform calculations for two open-shell atoms if one (or two) open shell(s) is (are) closed in the input data, our code can be used to calculate electron transitions for one open shell (or closed-shell noble gas atoms). The code has been tested by comparing its results with the photoionization cross sections of Ar $3p$ and O $2p$ electrons obtained from the computer program of [7]. Our method has been used to study the $4d$ giant resonances of Xe^+, I, and I^+.

We study the inner-shell electron transition from state $|l_1^{n_1}[L_1S_1]l_2^{n_2}[L_2S_2]LS\rangle$ to $|l_1^{n_1-1}[L_1'S_1']l_2^{n_2}[L_2S_2][L_c'S_c']l_3L'S'\rangle$, $l_1^{n_1}$ and $l_2^{n_2}$ are both open shells. L_c' and S_c' are, respectively, the core orbital and spin angular momenta. The RPAE equation we study here is similar to the equation found in [6,7],

$$\begin{aligned}
&\langle l_1^{n_1-1}[L_1'S_1']l_2^{n_2}[L_2S_2][L_c'S_c']l_3L'S'\|D\|l_1^{n_1}[L_1S_1]l_2^{n_2}[L_2S_2]LS\rangle \\
&\quad=\langle l_1^{n_1-1}[L_1'S_1']l_2^{n_2}[L_2S_2][L_c'S_c']l_3L'S'\|O^k\|l_1^{n_1}[L_1S_1]l_2^{n_2}[L_2S_2]LS\rangle+\sum_{L_c''S_c''}\sum_{\epsilon_4>F}[\langle l_1^{n_1-1}[L_1''S_1'']l_2^{n_2}[L_2S_2] \\
&\qquad\times[L_c''S_c'']l_4L''S''\|D\|l_1^{n_1}[L_1S_1]l_2^{n_2}[L_2S_2]LS\rangle\langle l_1^{n_1-1}[L_1'S_1']l_2^{n_2}[L_2S_2][L_c'S_c']l_3L'S'\|C\|l_1^{n_1-1}[L_1''S_1'']l_2^{n_2}[L_2S_2][L_c''S_c'']l_4L''S''\rangle/ \\
&\qquad(\omega-\epsilon_4+\epsilon_1+i\delta)-\langle l_1^{n_1}[L_1S_1]l_2^{n_2}[L_2S_2]LS\|D\|l_1^{n_1-1}[L_1''S_1'']l_2^{n_2}[L_2S_2][L_c''S_c'']l_4L''S''\rangle\langle l_1^{n_1-1}[L_1'S_1']l_2^{n_2}[L_2S_2] \\
&\qquad\times[L_c'S_c']l_3L'S';l_1^{n_1-1}[L_1''S_1'']l_2^{n_2}[L_2S_2][L_c''S_c'']l_4L''S''\|U\|l_1^{n_1}[\bar{L}_1\bar{S}_1]l_2^{n_2}[L_2S_2]\bar{L}\bar{S};l_1^{n_1}[\bar{L}_1\bar{S}_1]l_2^{n_2}[L_2S_2]\bar{L}\bar{S}\rangle/(\omega+\epsilon_4-\epsilon_1)], \qquad (1)
\end{aligned}$$

where the first term is the dipole matrix element in RPAE, the second term is the dipole matrix element calculated with Hartree-Fock (HF) wave functions. F is the Fermi level; ω, ϵ_1, and ϵ_4 are, respectively, the energies of the photon, l_1 and l_4 electrons. The infinitesimally small quantity $i\delta$ $(\delta\to 0)$ in the denominator determines the path to take in integrating the singular expressions in Eq. (1) over the continuous states. $\bar{L}_1$, $\bar{S}_1$, $\bar{L}$, and $\bar{S}$ represent any allowed $l_1^{n_1}$ subshell state and

the atomic state. In the calculation of the matrix elements a summation over these states has to be performed. O^k is the operator of the dipole matrix element, Eq. (4) of reference [8]. The Coulomb matrix elements of the first and second term in the bracket of Eq. (1) are, respectively the so-called "time-forward" type and "time-backward" type. The Coulomb matrix elements of the time-forward type can be obtained by the operator C, which equals $1/[L',S']^{1/2}$ times Eq. (17) of reference [8]. The Coulomb matrix elements of the time-backward type may be evaluated by using the operator U, which can be obtained after summing all the magnetic quantum numbers in Eq. (8) of reference [9].

All the matrix elements have been derived using the combined methods of the angular momentum theory, irreducible tensorial sets [10], tensorial products in a coupled form [8], coefficients of fractional parentage, second quantization [9], etc. The reduced dipole matrix element is given by

$$\langle L'S'|O^k|LS\rangle = \langle l_3\|C^k r\|l_1\rangle (-1)^{L'+k+L_2+L_1+S_c'+S_2+S_1+1/2+n_2}[L',L_c',L,S_c',L_1,S_1]^{1/2}\sqrt{n_1}G_{L_1'S_1'}^{L_1S_1} \times \begin{Bmatrix} L_1' & L_2 & L_c' \\ L & l_1 & L_1 \end{Bmatrix}\begin{Bmatrix} S_1' & S_2 & S_c' \\ S & 1/2 & S_1 \end{Bmatrix}\begin{Bmatrix} l_1 & k & l_3 \\ L' & L_c' & L \end{Bmatrix}, \tag{2}$$

where $G_{L_1'S_1'}^{L_1S_1}=(l_1^{n_1-1}\ [L_1'S_1']\}l_1^{n_1}[L_1S_1])$ is the fractional parentage coefficient, and C^k is nomalized spherical harmonics,

$$\langle l_3\|C^k\|l_1\rangle = (-1)^{l_3}[l_3,l_1]^{1/2}\begin{pmatrix} l_3 & k & l_1 \\ 0 & 0 & 0 \end{pmatrix}. \tag{3}$$

The symbols ( ) and { } in Eqs. (2) and (3) are the so-called $3j$ symbol and $6j$ symbol, respectively. The Coulomb matrix element of the time-forward type can be expressed as

$$\sum_{k\bar{L}\bar{S}\bar{L}_1\bar{S}_1} n_1[L_c'',L_c',S_c'',S_c']^{1/2}[\bar{L}_1,\bar{S}_1,\bar{L}]G_{L_1'S_1'}^{\bar{L}_1\bar{S}_1}G_{L_1''S_1''}^{\bar{L}_1\bar{S}_1}(-1)^{S_c''+S_c'+2S'+1}\begin{Bmatrix} l_3 & k & \bar{l}_1 \\ \bar{L} & L_c' & L' \end{Bmatrix}\begin{Bmatrix} l_1 & k & l_4 \\ L'' & L_c'' & \bar{L} \end{Bmatrix}\begin{Bmatrix} L_1'' & L_2 & L_c'' \\ \bar{L} & l_1 & \bar{L}_1 \end{Bmatrix}\begin{Bmatrix} S_1'' & S_2 & S_c'' \\ \bar{S} & 1/2 & \bar{S}_1 \end{Bmatrix}\begin{Bmatrix} \bar{L}_1 & L_2 & \bar{L} \\ L_c' & \bar{l}_1 & L' \end{Bmatrix}\begin{Bmatrix} \bar{S}_1 & S_2 & \bar{S} \\ S_c' & 1/2 & S_1' \end{Bmatrix}\langle l_4\|C^k\|l_1\rangle\langle \bar{l}_1\|C^k\|l_3\rangle R(l_4\bar{l}_1;l_1l_3) - \sum_{k\bar{L}\bar{S}\bar{L}_1\bar{S}_1} R(l_4\bar{l}_1;l_3l_1)\langle l_4\|C^k\|l_3\rangle \times\langle \bar{l}_1\|C^k\|l_1\rangle n_1[\bar{L}_1,\bar{S}_1,\bar{L},\bar{S}][L_c'',L_c']^{1/2}G_{L_1''S_1''}^{\bar{L}_1\bar{S}_1}G_{L_1'S_1'}^{\bar{L}_1\bar{S}_1}\begin{Bmatrix} L_c'' & l_4 & L'' \\ l_3 & L_c' & k \end{Bmatrix}\begin{Bmatrix} \bar{l}_1 & k & l_1 \\ L_c'' & \bar{L} & L_c' \end{Bmatrix}\begin{Bmatrix} L_1'' & L_2 & L_c'' \\ \bar{L} & l_1 & \bar{L}_1 \end{Bmatrix}\begin{Bmatrix} S_1'' & S_2 & S_2'' \\ \bar{S} & 1/2 & \bar{S}_1 \end{Bmatrix} \times\begin{Bmatrix} \bar{L}_1 & L_2 & \bar{L} \\ L_c' & \bar{l}_1 & L_1' \end{Bmatrix}\begin{Bmatrix} \bar{S}_1 & S_2 & \bar{S} \\ S_c' & 1/2 & S_1' \end{Bmatrix}(-1)^{l_4+L'+\bar{l}_1+L_c''+L_c'+\bar{L}+2S'+S_c''+2S_2+\bar{S}+1+\bar{S}_1+S_c'}, \tag{4}$$

where $R(l_4\bar{l}_1;l_1l_3)$ is the radial integral

$$R(l_4\bar{l}_1;l_1l_3) = \int R_{l_4}^* R_{\bar{l}_1}^* \frac{r_<^k}{r_>^{k+1}} R_{l_1}R_{l_3}r^2dr. \tag{5}$$

Before and after the minus sign in Eq. (4) are, respectively, the direct and exchange part of the Coulomb matrix element.

Similarly the Coulomb matrix element of the time-backward type can be evaluated using the following expression

$$\sum_{k\bar{L}\bar{S}\bar{L}_1\bar{S}_1} n_1[L_c'',L_c',S_c'',S_c']^{1/2}[\bar{L}_1,\bar{S}_1,\bar{L}]G_{L_1'S_1'}^{\bar{L}_1\bar{S}_1}G_{L_1''S_1''}^{\bar{L}_1\bar{S}_1}(-1)^{S_c''+S_c'+2S'+1}\begin{Bmatrix} l_3 & k & \bar{l}_1 \\ \bar{L} & L_c' & L' \end{Bmatrix}\begin{Bmatrix} l_1 & k & l_4 \\ L'' & L_c'' & \bar{L} \end{Bmatrix}\begin{Bmatrix} L_1'' & L_2 & L_c'' \\ \bar{L} & l_1 & \bar{L}_1 \end{Bmatrix}\begin{Bmatrix} S_1'' & S_2 & S_c'' \\ \bar{S} & 1/2 & \bar{S}_1 \end{Bmatrix} \times\begin{Bmatrix} \bar{L}_1 & L_2 & \bar{L} \\ L_c' & \bar{l}_1 & L' \end{Bmatrix}\begin{Bmatrix} \bar{S}_1 & S_2 & \bar{S} \\ S_c' & 1/2 & S_1' \end{Bmatrix}\langle l_4\|C^k\|l_1\rangle\langle l_3\|C^k\|\bar{l}_1\rangle R(l_4l_3;l_1\bar{l}_1) + \sum_{\bar{L}_1\bar{S}_1\bar{L}\bar{S}k} R(l_4,l_3,l_1,\bar{l}_1)\langle l_4\|C^k\|l_1\rangle \times\langle l_3\|C^k\|\bar{l}_1\rangle n_1[L_c'',S_c'',L_c',S_c]^{1/2}[\bar{L}_1,\bar{S}_1,\bar{L},\bar{S}]G_{L_1'S_1'}^{\bar{L}_1\bar{S}_1}G_{L_1''S_1''}^{\bar{L}_1\bar{S}_1}\begin{Bmatrix} L'' & L_c'' & l_4 \\ L_c' & \bar{L} & l_1 \\ l_3 & \bar{l}_1 & k \end{Bmatrix}\begin{Bmatrix} S_c' & 1/2 & S' \\ S_c'' & 1/2 & \bar{S}_1 \end{Bmatrix}\begin{Bmatrix} L_1'' & L_2 & L_c'' \\ \bar{L} & \bar{l}_1 & \bar{L}_1 \end{Bmatrix}\begin{Bmatrix} S_c' & S_2 & S' \\ \bar{S} & 1/2 & \bar{S}_1 \end{Bmatrix} \times\begin{Bmatrix} L_1' & L_2 & L_c' \\ \bar{L} & \bar{l}_1 & \bar{L}_1 \end{Bmatrix}\begin{Bmatrix} L_1' & L_2 & L_c' \\ \bar{L} & l_1 & \bar{L}_1 \end{Bmatrix}\begin{Bmatrix} S_1' & S_2 & S_c' \\ \bar{S} & 1/2 & \bar{S}_1 \end{Bmatrix}(-1)^{L_1''+L_1'+S_c'+S_c''+2\bar{S}_1+L_c'+L_c''+S_c'2S_2+2\bar{S}+1}, \tag{6}$$

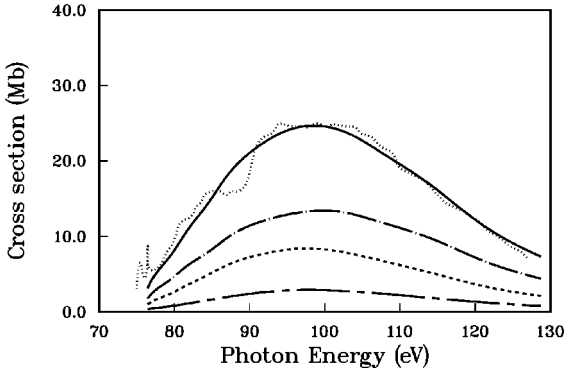

FIG. 1. Comparison of the RPAE results for the Xe^+ $4d$ giant resonance in the length form. The solid curve is the total photoionization cross section vs photon energy. The dashed, chan-dot, and chan-dash curves are, respectively, the ^2P, ^2D, and ^2S partial cross sections. The dotted curves represents the measured Xe^{3+} cross section from Ref. [12].

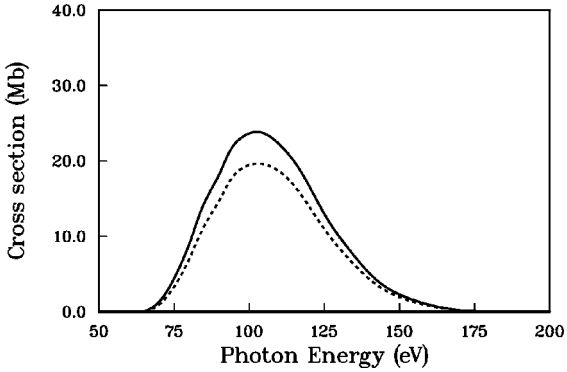

FIG. 2. The $4d$ giant resonance of the I atom. The solid and dotted curves represent our RPAE results in length and velocity forms, respectively.

where the symbol $\{\}$ with three lines in Eq. (6) is the so-called $9j$ symbol. Equations (2), (4), and (6) can be checked if l_1 and l_2 are set to represent closed shells. In this case, we have $\bar{L}_1=\bar{L}=0$, $\bar{S}_1=\bar{S}=0$, $L_1''=L_c''=l_1$, $S_1''=1/2$, $L_1'=L_c'=l_1$, $S_1,=1/2$, $L_2=0$, $S_2=0$, $L_c'=l_1$, $S_c'=S_1'=1/2$, $L_c''=l_1$, $S_c''=S_1''=1/2$, $S'=0$, and then the reduced dipole matrix element becomes the same as the equation for the closed shell atom. The reduced Coulomb matrix elements of the time-forward type and the time-backward type both become Eq. (4.55) of [11].

We have utilized our RPAE method to calculate the photoionization cross sections of the $4d$-ϵf transition, corresponding to the so-called giant resonances in Xe^+, I, and I^+.

We first create the ground state of Xe^+ $4d^{10}5s^25p^5(^2P)$ and the core wave functions of $4d^95s^25p^5(^1P,^1D,^1F,^3P,^3D,^3F)$ through self-consistent HF calculations. Then the radial functions of the continuum electron are obtained by solving the linear HF equations without self-consistency using those core wave functions. The reduced dipole matrix elements are evaluated using Eq. (2). As the core wave functions used relaxed orbitals, an overlap integral has to be added into the Eq. (2).

According to the triangular rule the final combined core and continuum electron states can only be ^2S, ^2P, and ^2D states. Therefore we included the following final states in the calculations: $4d^95s^25p^5(^1P)\epsilon f(^2D)$, $4d^95s^25p^5(^1D)\epsilon f(^2P,^2D)$, $4d^95s^25p^5(^1F)\epsilon f(^2S,^2P,^2D)$, $4d^95s^25p^5(^3P)\epsilon f(^2D)$, $4d^95s^25p^5(^3D)\epsilon f(^2P,^2D)$, $4d^95s^25p^5(^3F)\epsilon f(^2S,^2P,^2D)$, and studied the following reactions:

$$h\nu + 4d^{10}5s^25p^5(^2P) \rightarrow 4d^95s^25p^5(^1P,^1D,^1F,^3P,^3D,^3F) + \epsilon f(^2S,^2P,^2D). \quad (7)$$

After evaluating the matrix elements, Eq. (1) was solved to obtain the dipole matrix element in RPAE and the ^2S, ^2P, and ^2D partial cross sections. The total photoionization cross section is the sum of those partial cross sections. The photoionization of Xe^+ $4d$-ϵf is followed, with almost 100% probability, by a continuous double Auger decay process to the Xe^{3+} ion. Therefore, our calculaton can be compared with the Xe^{3+} measurement. Figure 1 shows the partial and total photoionization cross sections versus the photon energies for the Xe^+ $4d$-ϵf transition. The solid curve is the total photoionization cross section from the RPAE calculation in the length form. The dashed, chan-dot, chan-dash curves are, respectively, the results for the ^2P, ^2D, and ^2S partial cross sections. The dotted curve represents the measured Xe^{3+} cross section from reference [12]. The maximum cross section, 24.44 MB at the photon energy of 96.37 eV from our RPAE calculation agrees very well with the experimental maximum of 25 MB at the photon energy of 95 eV [12].

We also calculated the $4d$ giant resonances of I and I^+. The calculation for the I $4d$ to ϵf transition is similar to that for the Xe^+ case except that the two elements have different nuclear charges. Figure 2 represents the $4d$ giant resonance of the I atom. The solid and dashed curves are, respectively, the length and velocity forms of our RPAE calculation. They have maxima at 102.8 eV of 23.85 MB (length) and 19.6 MB (velocity), which agree reasonably well with the results of the time-dependent local-density approximation (TDLDA) [13]. TDLDA predicts a peak at 96 eV with a maximum value of 27 Mb. However, our data show about three to four times higher than the experimental maximum of 6.5 MB at 91 eV [14]. Since the recent measurement for I^+ $4d$ giant resonance shows a maximum of 23 ± 3 Mb at 90 eV [15], we recommend a remeasurement of the I $4d$ giant resonance with a careful experimental arrangement.

For the I^+ $4d$ giant resonance the ground state is $4d^{10}5s^25p^4(^3P)$ while the core wave functions are $4d^95s^25p^4(^2P,^2D,^2F)$ and $4d^95s^25p^4(^4P,^4D,^4F)$. We have included the following final combined core and continuum electron states in the calculations: $4d^95s^25p^4(^2P)\epsilon f(^3D)$, $4d^95s^25p^4(^2D)\epsilon f(^3P,^3D)$, $4d^95s^25p^4(^2F)\epsilon f(^3S,^3P,^3D)$, $4d^95s^25p^4(^4P)\epsilon f(^3D)$, $4d^95s^25p^4(^4D)\epsilon f(^3P,^3D)$, $4d^95s^25p^4(^4F)\epsilon f(^3S,^3P,^3D)$. Therefore the reactions we studied are

$$h\nu + 4d^{10}5s^25p^4(^3P) \rightarrow 4d^95s^25p^4(^2P,^2D,^2F,^4P,^4D,^4F) + \epsilon f(^3S,^3P,^3D). \quad (8)$$

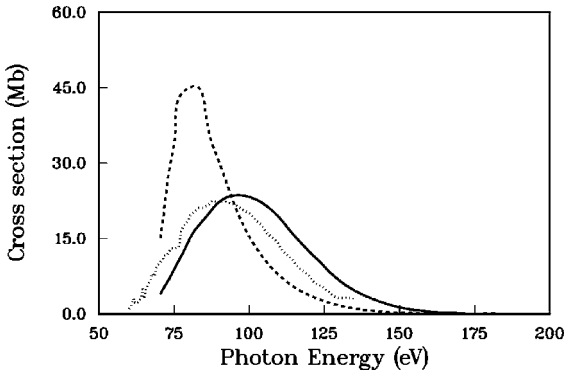

FIG. 3. Comparison of RPAE and HF calculations of the I^+ 4*d* giant resonance with the experimental data. The solid and dashed curves are our RPAE and HF calculations, respectively. The dotted curves are the experimental results.

We obtained the total photoionization cross section from the sum of the partial cross sections for ^3S, ^3P, and ^3D. Figure 3 shows the total photoionization cross sections for the 4*d* giant resonance of I^+. The solid and dashed curves are, respectively, the length results from our RPAE and HF calculations. The dotted curve represents the experimental data [15]. The RPAE curve gives a maximum of 23.59 Mb at the photon energy of 95.62 eV, which agrees very well with the recent measurement, 23(±3) Mb at 90 eV [15]. The importance of the RPAE effects are clearly manifested through the comparison with the HF results.

Calculated photoionization cross sections (MB) versus photon energies for the $4d$-ϵf giant resonance of the ions Xe^+ and I^+, and atom I are given in Table I.

In summary, a RPAE method has been developed and used to study the 4*d* giant resonances of Xe^+, I, and I^+. The present photoionization cross sections for Xe^+ and I^+ agree very well with the experimental data. However, the results for the I 4*d* giant resonance are about three to four times higher than those from the measurement [14]. We recommend a remeasurement of the cross section for this process.

TABLE I. Photoionization cross sections (MB) calculated by our RPAE method for the $4d$-ϵf giant resonance of the ions Xe^+ and I^+ and the atom I.

Photon (eV)	Xe^+	Photon (eV)	I^+	Photon (eV)	I
76.46	3.09	70.46	3.86	65.31	0.11
76.80	3.87	70.80	4.30	65.65	0.15
77.76	5.35	71.76	5.32	66.61	0.29
79.33	7.26	73.33	6.87	68.18	0.67
81.52	10.51	75.52	9.41	70.37	1.47
84.31	14.18	78.31	12.53	73.16	3.07
87.72	18.89	81.72	16.45	76.57	5.69
91.74	22.33	85.74	19.32	80.59	9.58
96.37	24.44	90.38	22.42	85.22	14.57
101.62	24.20	95.62	23.59	90.47	18.60
107.48	21.12	101.48	22.92	96.33	22.74
113.95	16.88	107.95	20.38	102.80	23.85
121.03	11.48	115.03	15.52	109.88	22.27
128.73	7.32	122.73	10.75	117.57	18.36
137.03	3.91	131.03	6.15	125.88	12.39
145.95	1.94	139.95	3.22	134.80	7.50
155.48	0.74	149.48	1.34	144.33	3.60
165.62	0.21	159.63	0.46	154.47	1.58
176.38	0.016	170.38	0.074	165.23	0.47
187.75	0.035	181.75	0.0093	176.60	0.06

This work was supported by the U.S. DOE, Division of Chemical Sciences, Geosciences and Biosciences, Office of Basic Energy Sciences, OER, and AFOSR.

[1] E. Dalgaard, J. Phys. B **8**, 695 (1975).
[2] L. Armstrong, Jr., J. Phys. B **7**, 2320 (1974).
[3] A. F. Starace and L. Armstrong, Jr., Phys. Rev. A **13**, 1850 (1976).
[4] D. J. Rowe, Rev. Mod. Phys. **40**, 153 (1968).
[5] N. A. Cherepkov and L. V. Chernysheva, Biol. Bull. Acad. Sci. USSR **41**, 47 (1977).
[6] G. A. Vesnicheva *et al.*, Sov. Phys. Tech. Phys. **31**, 402 (1986).
[7] M. Ya. Amusia and L. V. Chernysheva, *Computation of Atomic Processes* (IOP, Bristol, 1998).
[8] P. H. M. Uylings, J. Phys. B **25**, 4391 (1992).
[9] B. R. Judd, *Second Quantization and Atomic Spectroscopy* (Johns Hopkins Press, Baltimore, MD, 1967).
[10] U. Fano and G. Racah, *Irreducible Tensorial Sets* (Academic, New York, 1959).
[11] M. Ya. Amusia, *Atomic Photoeffect* (Plenum, New York, 1990).
[12] P. Andersen, T. Andersen *et al.*, J. Phys. B **34**, 2009 (2001).
[13] G. O'Sullivan *et al.*, Phys. Rev. A **53**, 3211 (1996).
[14] L. Nahon *et al.*, Phys. Rev. A **43**, 2328 (1991).
[15] H. Kjeldsen *et al.*, Phys. Rev. A **62**, 020702(R) (2000).